Ce L_{III}-edge X-ray Absorption Spectroscopic Studies on the Tetrameric Ce-polyoxyhydroxy Cation Intercalated Aluminosilicate

Joo-Byoung Yoon, Sung-Ho Hwang, Dong-Kuk Kim,† Seong-Gu Kang,‡ and Jin-Ho Choy*

National Nanohybrid Materials Laboratory and School of Chemistry and Molecular Engineering, Seoul National University, Seoul 151-742, Korea
†Department of Chemistry, College of Natural Sciences, Kyungpook National University, Daegu 702-701, Korea
‡Division of Material and Chemical Engineering, College of Engineering, Hoseo University, Chung-Nam 336-795, Korea
Received December 2, 1999

The cerium ion intercalated aluminosilicate was prepared by ion exchange reaction between Na^+ in montmorillonite and Ce^{4+} in aqueous solution. The X-ray absorption near edge structure (XANES) analyses indicate that the Ce^{4+} ions are partially reduced to the Ce^{3+} ones during the intercalation into layered aluminosilicate due to a charge transfer between host and intercalant. From the EXAFS analysis, two different (Ce–O) bonding pairs could be characterized with the distances and coordination numbers of 2.31 (±0.02) Å × 8.2 (±1.5) and 2.66 (±0.02) Å × 2.7 (±1.0), respectively, with the oxygen atoms as the first nearest neighbor, and two (Ce–Ce) pairs at 3.78 Å as the second neighbor. It is therefore concluded that the most probable Ce-species stabilized in the interlayer space of aluminosilicate after the intercalation is the tetrameric Ce-polyoxy/hydorxy cations with the mixed valent state of 0.75 Ce^{4+}/0.25 Ce^{3+}.

Introduction

Recently, two-dimensional (2-D) materials have attracted intense research interest due to their applicability in preparing highly porous nanocomposites with selective catalytic activity and with molecular adsorption and sieving capacity.[1-3] Moreover, the porous layered clays pillared with rare earth elements have also been studied not only to improve the catalytic activity and thermal stability,[4-6] but also to understand the relation between the electronic structure of mixed valent rare earth cation and the physico-chemical properties such as solid acid catalysis and radioactive nuclear waste repositories.[7,8]

Since the layered materials and their intercalates are highly anisotropic and poor in crystallinity, the conventional diffraction techniques may not provide their detailed structural information. In this regard, the extended X-ray absorption fine structure (EXAFS) and X-ray absorption near edge structure (XANES) spectroscopies are the most powerful tool in determining the electronic and geometric structures of ions, molecules, and condensed matters, whatever those are crystalline or amorphous isotropic or not.[9] Especially, in the structural characterization of silicate intercalation complexes, the much lower contribution to the absorption coefficient of the lighter element like Si, Al and Mg in the silicate matrix can provide very good sensitivity to the intercalated heavy element even though those are in minor concentration.[9-11]

In the present study, an attempt has been made to intercalate cerium ions into layered silicate, montmorillonite, and to analyze the local structure and valence state of cerium ions stabilized in the interlayer space by X-ray absorption spectroscopy (XAS).

*Authors to whom correspondence should be addressed. E-mail: jhchoy@plaza.snu.ac.kr, Tel: +82-2-880-6658, Fax: 82-2-872-9864

Experimental Section

Sample preparation. The particle size of the starting material of montmorillonite (Junsei Chem. Co.) was controlled to < 0.2 μm with a sedimentation-fractionation technique, and no impurities of other materials were found in the X-ray diffraction (XRD) analysis. The chemical formula of $Na_{0.40}(Fe_{0.19}Mg_{0.26}Al_{1.60})(Si_{3.88}Al_{0.12})O_{10}(OH)_2$ and cation exchange capacity (CEC) of ~100 meq/100 g were determined, respectively, by inductively coupled plasma (ICP) and CEC measurement.

A saturated aqueous solution of $Ce(SO_4)_2 \cdot 4H_2O$ and 1 wt% dispersed montmorillonite suspension were used for the ion exchange reaction, which was performed at room temperature for 3 hours. The cerium ion exchanged clays were centrifuged and washed with deionized water until the clay suspension gave colorless supernatant, indicating the removal of all the cerium species attached on the clay surface. The obtained Ce-montmorillonite was freeze-dried at room temperature for 1 hour and used for further analyses.

Characterization. Powder XRD measurements were made on a JEOL-JDX diffractometer with Ni-filtered Cu K_α radiation (λ = 1.54184 Å) and the amounts of metallic species were determined with Shimazu ICP spectrometer (ICPS-5000).

X-ray absorption measurements were carried out with synchrotron radiation with the EXAFS facility installed at the beam line 7C of the Photon Factory, the National Laboratory for High Energy Physics (Tsukuba), operated at 2.5 GeV with *ca.* 350-400 mA of stored current. The Ce L_{III}-edge XAS was taken in a transmission mode using ionization chambers filled with N_2 (I_0) and N_2 + Ar (I_t) at room temperature, using a Si(111) double crystal monochromator. To remove the higher harmonic oscillation effect, the intensity was detuned by

30% of the maximum of the incident beam. To ensure the spectral reliability, much care has been taken to evaluate the stability of the energy scale by monitoring the spectrum of cerium oxide for each measurement and thus edge positions were reproducible to be better than 0.05 eV.

XANES and EXAFS data analyses. The data analyses for experimental spectra were performed by the standard procedure as previously described.[12-14] Photon energies of all XANES spectra were calibrated by the first absorption peak in the CeO_2 one, defined at 5723.4 eV. The inherent background in the data was removed by fitting a polynomial to the pre-edge region and extrapolating it through the entire spectrum, from which it was subtracted. The absorbance μ(E) was normalized to an edge jump of unity for comparing the XANES features directly to one another. Nonlinear least-squares EXAFS curve fitting between the experimental EXAFS spectrum and the theoretical one calculated by *ab-initio* FEFF6 code[15,16] was carried out by UWXAFS2.0 code,[17] and the structural parameters such as coordination number (N), bond distance (R_i), Debye-Waller factor (σ_i^2), and threshold energy difference (ΔE_0) were optimized as variables.

Results

Powder XRD. The intercalation of Ce^{4+} ions into montmorillonite was confirmed by powder XRD as shown in Figure 1. The (001) peak at 2θ=5.9° gives the basal spacing of d = 14.98(±0.05) Å, which allows us to estimate the size (5.4 Å) of intercalant cerium species by subtracting 9.6 Å of the thickness of the silicate layer form the observed *d*-spacing. The powder XRD pattern for the heat-treated Ce-montmorillonite at 250 °C shows the basal spacing of 13.8 Å, even though the crystallinity is highly reduced, contrast to Na-montmorillonite which shows the basal spacing of 9.6 Å after heating at 250 °C. These layer distances suggest that the intercalated cerium species is not consistent with that of the hydrated cerium ion but probably with that of a large sized cerium oligomer, considering the ionic size of Ce^{4+} of 0.87-1.14 Å with the coordination numbers of 6-10.[18] This fact is well consistent with following XANES and EXAFS results. However, the Ce-montmorillonite becomes X-ray amorphous after the heat-treatment beyond 300°C.

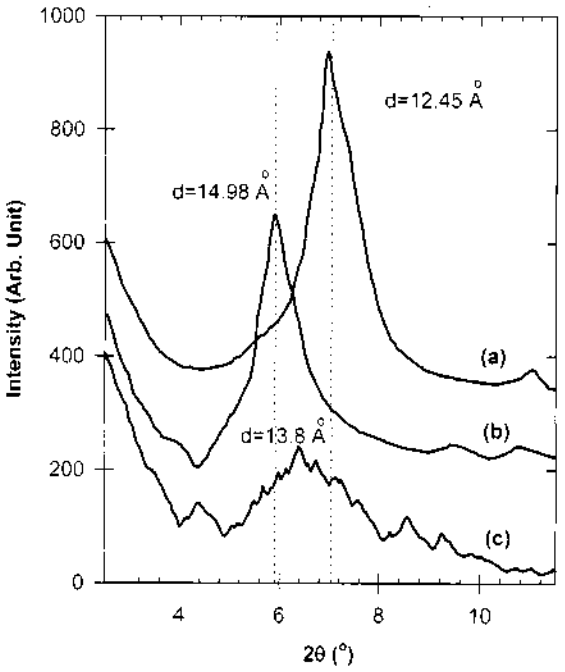

Figure 1. Powder X-ray diffraction patterns for (a) Na-montmorillonite, (b) Ce-montmorillonite, and (c) Ce-montmorillonite heat-treated at 250 °C.

XANES spectra. Figure 2 shows the Ce L_{III}-edge XANES spectra for the Ce-montmorillonite and reference compounds such as $Ce(SO_4)_2{\cdot}4H_2O$ and $Ce_2(SO_4)_3{\cdot}8H_2O$ with the tetravalent ceric and trivalent cerous ions, respectively. Though $Ce_2(SO_4)_3{\cdot}8H_2O$ shows a single peak (B) around 5727 eV in the XANES spectrum, $Ce(SO_4)_2{\cdot}4H_2O$ with the Ce^{4+} ion shows a remarkable splitting (about 7 eV) of the white line caused by two different configurations in the initial state.[19-21] In general, the broad peak D is assigned to the Ce $[2p^54f^05d^{*1}]$ O$[2p^6]$ final state configuration (possibly with some weak contribution of the Ce$[2p^54f^25d^{*1}]$ O$[2p^4]$) and the peak C to the Ce$[2p^54f^15d^{*1}]$. A distinct energy difference between the peaks B and C was observed as much as 4 eV as previously described.[22-23] On the other hand, in the case of Ce-montmorillonite, the peak C shifts to a lower energy side of 1.5 eV with a slight suppression of the peak D without any energy shift, indicating the stabilization of trivalent cerium ions in the interlayer space of montmorillonite. The spectrum of $Ce(SO_4)_2{\cdot}4H_2O$ shows also a shoulder (A) around

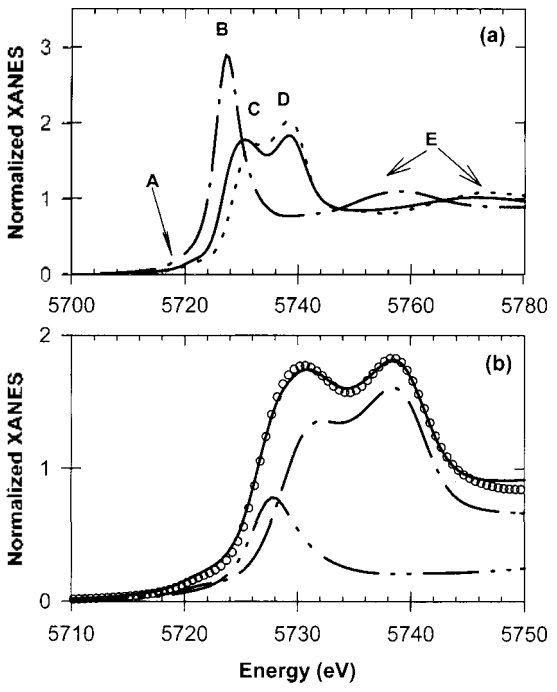

Figure 2. (a) Ce L_{III}-edge XANES spectra for Ce-montmorillonite (—) and reference compounds, $Ce(SO_4)_2{\cdot}8H_2O$ (——) and $Ce_2(SO_4)_3{\cdot}4H_2O$ (–·–) (b) Ce L_{III}-edge XANES spectra for Ce-montmorillonite (open circles) and the simulated XANES spectrum (—) based on the weight factor of 0.75 for $Ce(SO_4)_2{\cdot}4H_2O$ (–·–) and 0.25 for $Ce_2(SO_4)_3{\cdot}8H_2O$ (–··–)

5720 eV in the near of absorption edge which can be assigned to the transitions to the bottom of conduction band.[24]

And a broad feature over 5750 eV denoted as the peak E can be explained by multiple scattering (MS) effects due to the penetration of EXAFS at continuum state which shows the higher energy shift as much as 15 eV in the Ce^{4+} compound, compared to the Ce^{3+} one. It is well known that the MS peak position is highly related to the bond distance between central atom and the first nearest neighbors,[25-26] since the shorter the distance is, the higher the peak energy becomes. Therefore, a slight low energy shift in Ce-montmorillonite complex compared to that in $Ce(SO_4)_2{\cdot}4H_2O$ is an indication that the (Ce–O) bond distance would be slightly elongated, which is well consistent with the formation of trivalent cerous species as found in the above XANES results.

A shoulder peak occasionally observed in XANES spectrum of CeO_2, due to the presence of a small amount of Ce^{3+} with the configuration of $4f^1$, was not observed in $Ce(SO_4)_2{\cdot}4H_2O$, and no double-peak in $Ce_2(SO_4)_3{\cdot}8H_2O$ indicates the purity of reference compounds. Therefore, it becomes possible to estimate the contribution of Ce^{3+}/Ce^{4+} to the entire XANES spectrum of the Ce-montmorillonite. Figure 2b shows the simulated spectrum by assuming the weight factors of 0.75 for Ce^{4+} and 0.25 for Ce^{3+}, respectively. The overall shape of simulated spectrum shape could be reproducibly represented, and is in good agreement with experimental one, indicating a charge transfer from the montmorillonite lattice to the intercalant cerium complex as found in various intercalation compounds.

EXAFS spectra. Figure 3 shows the k^2-weighted EXAFS oscillations and their Fourier transforms (FTs) in the range of ~1.5 $Å^{-1}$ < k < 10.0 $Å^{-1}$. The first peak around 2.0 Å is due to the first oxygen ligands, and the next peak around ~3.5 Å corresponds to the outer Ce---Ce or Si shells. It is important to note here that the cerium species intercalated show a characteristic feature in FTs. The first is a strong reduction of the intensity in the first neighbor region compared to that of the trivalent or tetravalent Ce sulfate salt and the second is an enhancement of the intensity in the second neighbors region around 3.5 Å, as indicated by an arrow in Figure 3b.

For the quantitative analysis of the structural data, a nonlinear least squares curve fitting was carried out for reference compounds, $Ce(SO_4)_2{\cdot}4H_2O$ and $Ce_2(SO_4)_3{\cdot}8H_2O$. The best-fitted structural parameters are summarized in Table 1,

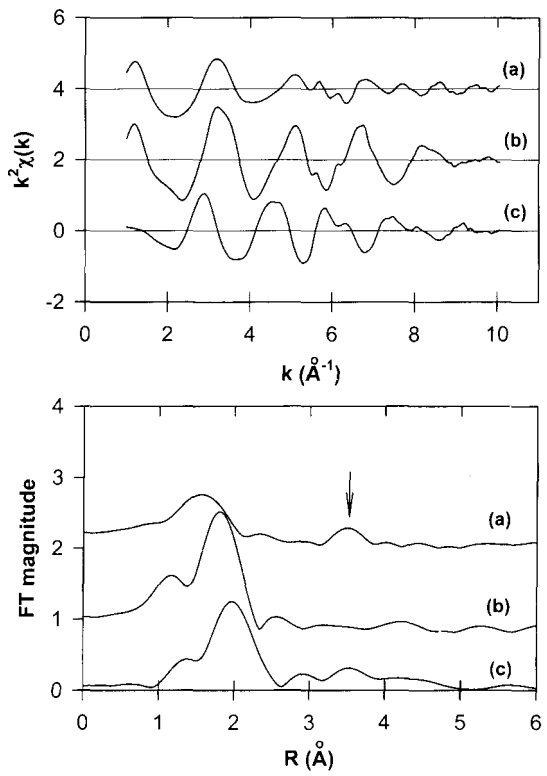

Figure 3. The k^2-weighted EXAFS oscillations (top) and their Fourier transforms (bottom) for the first shell. (a) Ce-montmorillonite, (b) $Ce(SO_4)_2{\cdot}4H_2O$, and (c) $Ce_2(SO_4)_3{\cdot}8H_2O$.

and the inverse FTs and $k^2\chi(k)$ for the first shell are compared with theoretical spectra depicted by using the parameters obtained (Figure 4). The best-fitted distances are in good agreement with the crystallographic values within the experimental error limit (±0.02 Å).[27,28]

The first shell-fitting result for the Ce-montmorillonite complex shows the two oxygen shells with the distance difference of 0.35 Å which destructively interfere with each other, leading to a large suppression of the FT amplitude as shown in Figure 4. It should be noted that the Debye-Waller factors for (Ce–O) bonding pairs, reflecting on static/dynamic disorder are largely increased after the intercalation. Such a fact represents the large disorder in bond distance compared to those of the reference compounds. A small increase of 0.07 Å in average bond distance after the intercalation, compared to the tetravalent reference compound $Ce(SO_4)_2{\cdot}4H_2O$

Table 1. EXAFS fitting results for Ce-montmorillonite and reference compounds[a]

Compounds	Bonding pairs	CN[b]	R (Å)[b]	E_0 (eV)	σ^2 ($\times10^{-3}$ Å^2)	R factor
Ce-Mont.	Ce–O1	8.2	2.31_4	-1.73	26.76	0.006
	Ce–O2	2.7	2.66_1	"	11.2	0.006
	Ce–Ce[c]	2.4	3.78_1	-1.83	5.17	0.047
$Ce_2(SO_4)_3{\cdot}8H_2O$	Ce–O	8.2 (7.5)	2.54_0 (2.55_2)	-6.31	7.18	0.007
$Ce(SO_4)_2{\cdot}4H_2O$	Ce–O	8 (8)	2.33_2 (2.32_6)	0.63	3.91	0.015

[a]The fitting ranges for k and R are 1.5-9.5 $Å^{-1}$ and 0.50-2.65 Å, respectively and the independent points are 8. Errors for CN (coordination number) and σ^2 (Debye-Waller factor) are 20%, and those for R (interatomic distance) and E_0 (threshold energy difference) are 0.02 Å and 1.8 eV, respectively. [b]The R values and coordination numbers for Ce^{3+} and Ce^{4+} in parenthesis are from references (12) and (13), respectively. [c]These values are obtained from k^3-weighted EXAFS signal of k = 3.0-10.0 $Å^{-1}$ and R = 3.0-4.1 Å.

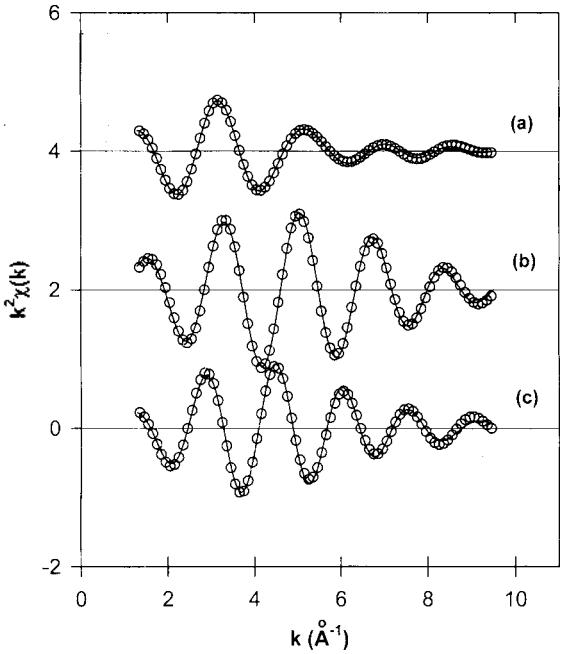

Figure 4. The Fourier filtered EXAFS oscillations (solid line) and their fitting results (open circles) for the first shell. (a) Ce-montmorillonite, (b) $Ce(SO_4)_2{\cdot}4H_2O$, and (c) $Ce_2(SO_4)_3{\cdot}8H_2O$.

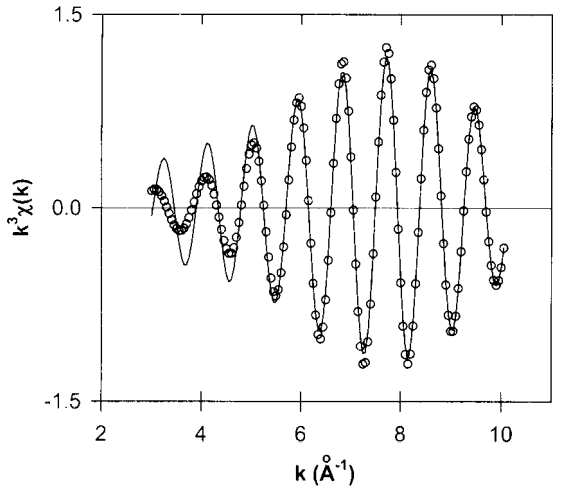

Figure 5. The second shell fitting results for Ce-montmorillonite.

underlines the formation of Ce^{3+} in the intercalation complex as observed in the XANES spectra.

The second shell around 3.5 Å was fitted with the outer Ce---Ce pair as shown in Figure 5 and the fitting results are summarized in Table 1. The fits for the second neighbors with Si standard were also carried out, but it did not give any physically reasonable structural parameters. The magnitude of envelop in Figure 5 shows a maximum around 8 Å^{-1} which indicates the presence of heavy metal species as a second neighbor. A small difference in low k region is probably due to the penetration of the oscillation of the first oxygen shell or due to the possible Si pairs, but it was impossible to do curve-fit using further shells (*i.e.* including Si neighbors) since the number of the independent points was too small to carry out such curve-fits.

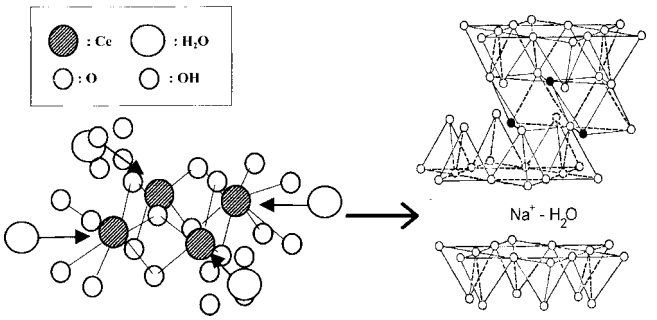

Figure 6. The schematic descriptions of the tetrameric cerium oxy/hydroxy polycation and montmorillonite.

Discussion

On the basis of EXAFS fitting results, it is possible to propose the structural model for the cerium species in the interlayer space of clay as shown in Figure 6. It is interesting to point out that the hexamer polycation of $[Ce_6(\mu_4\text{-}O)_4(\mu_3\text{-}OH)_4(H_2O)_{24}]^{12+}$ could be formed in an acidic aqueous media of which cerium atoms are in an eight fold coordinated oxygen ligand field (antiprism) composed of four water molecules at 2.6 Å and the other four oxygen atoms of μ_{oxo} and $\mu_{hydroxo}$ at 2.21 Å and 2.46 Å, respectively.[29] The distance between Ce---Ce is 3.77 Å in the polycation which is identical with the present EXAFS result of 3.78 Å. It was also reported that the tetrameric unit of $Ce_4(\mu_4\text{-}O)(\mu_3\text{-}OH)(acac)_{12}$ as intermediates of hexamer could be formed in the course of the hydrolysis of cerium isopropoxide in the acetylacetonate medium,[30] of which interatomic distance is very similar to that obtained from present EX AFS results. Considering the molecular dimension of hexameric species and tetrameric one, the gallery height of 5.3 Å confirms that the cerium species in interlayer region is the tetrameric form, not the hexameric one. Therefore, it is suggested that the tetrameric Ce-polyoxy/hydorxy cations are stabilized in the interlayer space of two-dimensional silicate layers after the intercalation.

Conclusion

In the present study, the local structure and valence state of cerium ion intercalated in montmorillonite have been investigated by X-ray absorption spectroscopy. According to the XANES spectroscopy, it is confirmed that about 25% Ce^{4+} was reduced into Ce^{3+} after the intercalation, which is consistent with the EXAFS results representing the longer (Ce-O) bond distance of 0.07 Å. The three cerium atoms are also observed at 3.78 Å as second neighbors. It is therefore suggested that the tetrameric Ce-polyoxy/hydorxy cations arestabilized in the interlayer space of two-dimensional silicate layers after the intercalation.

Acknowledgment. Financial support in part from the Brain Korea 21 program is gratefully acknowledged. Authors are grateful to Prof. M. Nomura for helping us to get the XAS data in the Photon Factory.

References

1. Bruch, R. *Catalysis Today* **1988**, *2*, 1.
2. Corma, A. *Chem. Rev.* **1997**, *97*, 2373.
3. Choy, J.-H.; Park, J.-H.; Yoon, J.-B. *J. Phys. Chem.* **1998**, *102*, 5991.
4. Zhao, D.; Yang, Y.; Guo, X. *Mat. Res. Bull.* **1993**, *28*, 939.
5. Kloprogge, J. T.; Breukelaar, J.; Geus, J. W.; Jansen, J. B. H. *Clays and Clay Minerals* **1994**, *42*, 18.
6. Munoz-Paez, A.; Alba, M. D.; Castro, M. A.; Alvero, R.; Trillo, J. M. *J. Phys. Chem.* **1994**, *98*, 9850.
7. Tsunashima, A.; Brindley, G. W.; Bastovanov, M. *Clays and Clay Minerals* **1981**, *29*, 10.
8. Tokarz, M.; Shabtai, J. *Clays and Clay Minerals* **1985**, *33*, 89.
9. Choy, J.-H.; Kim, D.-K.; Park, J.-C.; Choi, S.-N.; Kim, Y.-J. *Inorg. Chem.* **1997**, *36*, 189.
10. Michalowicz, A.; Verdaguer, M.; Mathey, Y.; Clement, R. *Synchrotron Radiation in Chemistry and Biology I*; Mandelkow, E., Ed.; Springer-Verlag: Berlin, 1988; pp 107-149.
11. Berry, F. J.; Marco, J. F.; Steel, A. T. *Zeolites* **1994**, *14*, 344.
12. Teo, B. K. *EXAFS: Basic Principles and Data Analysis*; Springer-Verlag: Berlin, 1986; pp 114-157.
13. *X-ray absorption. Principles, applications, techniques of EXAFS, SEXAFS, and XANES*; Konigsberger, D. C., Prins, R., Eds.; Wiley: New York, 1988; pp 444-457.
14. Lytle, F. W. *Applications of Synchrotron Radiation*; Winick, H., Xian, D., Huang, M., Ye, T., Eds.; Gordon and Breach: 1989; pp 135-223.
15. Rehr, J. J. *Jpn. J. Appl. Phys.* **1993**, *32*, 8.
16. Rehr, J. J.; Zabinsky, S. I.; Albers, R. C. *Phys. Rev. Lett.* **1992**, *69*, 3397.
17. Stern, E. A.; Newville, M.; Ravel, B.; Yacoby, Y.; Haskel, D. *Physica B* **1995**, *208&209*, 117.
18. Shannon, R. D. *Acta Crystallogr.* **1976**, *A32*, 751.
19. Dexpert, H.; Karnatak, R. C.; Esteva, J. -M.; Connerade, J. P.; Gasgnier, M.; Caro, P. E. Albert, L. *Phys. Rev. B* **1987**, *36*, 1750.
20. Bianconi, A.; Marcelli, A.; Tomellini, M.; Davoli, I. *J. Mag. & Mag. Mater.* **1985**, *47&48*, 209.
21. Bianconi, A.; Marcelli, A.; Dexpert, H.; Karnatak, R.; Kotani, A.; Jo, T.; Petiau, J. *Phys. Rev. B* **1987**, *35*, 806.
22. Sham, T. K. *Phys. Rev. B* **1989**, *40*, 6045.
23. Prieto, C.; Lagarde, P.; Dexpert, H.; Priois, V.; Villain, F.; Verdaguer, M. *J. Phys. Chem. Solids* **1992**, *53*, 233.
24. Soldatov, A. V.; Ivanchenko, T. S.; Longa, S. D.; Kotani, A.; Iwamoto, Y.; Bianconi, A. *Phys. Rev. B* **1994**, *50*, 5074.
25. Garcia, J.; Benfatto, M.; Natoli, C. R.; Bianconi, A.; Fontaine, A.; Tolentino, H. *Chem. Phys.* **1989**, *132*, 295.
26. Sham, T. K. *J. Chem. Phys.* **1983**, *79*, 1116.
27. Lindgren, O. *Acta Chem. Scand.* **1977**, *A31*, 453.
28. Caminiti, R.; Cucca, P.; D'Andrea, A. *Z. Naturforschung* **1983**, *38a*, 533.
29. Sanchez, C.; Toledano, P.; Ribot, F. *Mat. Res. Soc. Symp. Proc.* **1990**, *180*, 47.
30. Ribot, F.; Toledano, P.; Sanchez, C. *Chem. Mater.* **1991**, *3*, 759.